Vol. 13 (2020) *Acta Physica Polonica B Proceedings Supplement* No 4

CHARGE STATE EVOLUTION IN ELECTRON BEAM ION TRAP*

W. Biela, A. Warczak, A. Mucha, A. Malarz

M. Smoluchowski Institute of Physics, Jagiellonian University
Łojasiewicza 11, 30-348 Krakow, Poland

(Received February 27, 2020)

Recently, at the M. Smoluchowski Institute of Physics of the Jagiellonian University a commercial electron beam ion trap (EBIT) was installed for teaching and scientific purposes. The first experiments were focused on observation of radiative recombination and dielectronic recombination. An investigation of higher order resonant recombination processes was also initiated. These recombination processes depend strongly on the charge state of the ions involved in these processes. The EBIT plasma contains always a mixture of different charge states. Therefore, the charge-state distribution of the ions is crucial for the observed atomic processes. A new diagnostics tool for this distribution and a possibility of its manipulation form the main goal of the present paper which may help to better understand the processes investigated with an EBIT.

DOI:10.5506/APhysPolBSupp.13.975

1. Introduction

An electron beam ion trap (Dresden EBIT [1, 2], DREEBIT Co.), equipped with an X-ray detector (XFlash 5030, Bruker Co.), opens a wide range of possibilities for studies of atomic processes associated with ion production and trapping in an EBIT [2]. The starting experiments were dedicated to the most simple type of recombination process called radiative recombination (RR). In this case, capture of a free electron into a bound state of an ion is accompanied by the emission of a photon. The energy of this photon is equal to the change of the electron energy shown in the inset of Fig. 1. RR may be considered as the time reversal of photoionization. The RR concerns K-, L- and higher shells. It is also possible that the interaction between ion and a free electron causes change of the electron kinetic energy without

* Presented at the 45$^{\text{th}}$ Congress of Polish Physicists, Kraków, September 13–18, 2019.

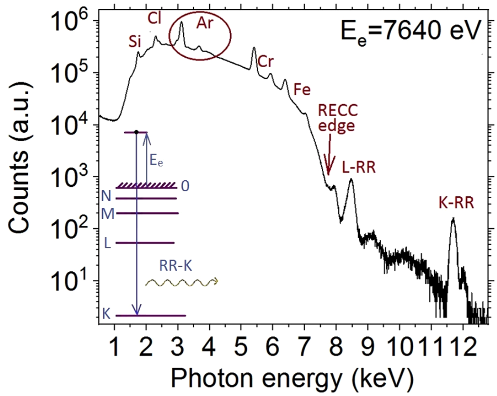

Fig. 1. A typical spectrum observed in the EBIT for Ar ions at electron energy (E_e) of 7640 eV, inset explains RR transitions.

its binding into a bound state of the ion. This process produces a continuum spectrum of radiation called Radiative Electron Capture to Continuum (RECC, also called bremsstrahlung). A sharp edge at photon energy equal to the electron beam energy is a characteristic feature of RECC (Fig. 1). Resonant recombination processes, involving more than one electron, have also been already observed in the Jagiellonian EBIT laboratory. The most basic of these resonant processes is dielectronic recombination (DR) where a free electron is captured into a bound state of an ion with the simultaneous excitation of a core electron [3–6]. The multi-electron resonant processes, like DR, are governed by the electron–electron interaction and are of great importance in plasmas, not only in EBIT [3–8], but also in astrophysical settings [9] and nuclear fusion plasmas [10, 11]. Therefore, the DR process was a subject of intense investigations with the use of ion traps [3–8] and accelerators [12, 13]. Moreover, DR is also important for nuclear physics as it enables nuclear structure testing [14]. In addition, a detailed study of electron correlations, which govern multi-electron processes, may give a sensitive test for quantum electrodynamics [14–16]. A detailed explanation of multi-electron resonant processes requires a deep understanding of the charge-state distribution in order to point the active ions.

In the EBIT plasma, a mixture of different charge states is always present. The charge-state distribution depends on many EBIT parameters such as: electron energy, electron current, ionization time, gas pressure and trapping potential [1, 2]. Since the multi-electron resonant processes are strongly dependent on the electron configuration of the ion, it is necessary to optimize the above-mentioned EBIT parameters in order to obtain the optimal charge-state distribution and to enhance the expected processes. This task can be solved by means of a specific tool which would help us to perform the diagnosis of the current charge-state distribution of the ions in the EBIT plasma. In this paper, we propose, as this tool, the charge-state distribution analysis based on the deconvolution of the K_α line profile. In order to perform this deconvolution, we need a properly simulated profiles of the K_α line for different charge states. Here, the Flexible Atomic Code (FAC) [17] is used for conducting these calculations. One should stress that this procedure may be used in many EBIT experiments in order to prepare the dominant charge-state component in the ions mixture, which is preferred by the investigated process.

2. Electron beam ion trap

A standard EBIT from the DREEBIT Co. [1, 2] (with data-collecting software) is being used to conduct the experiments. It is a compact apparatus that enables production and trapping of highly-charged ions (Fig. 2). The electron beam is emitted by a high current cathode and guided through

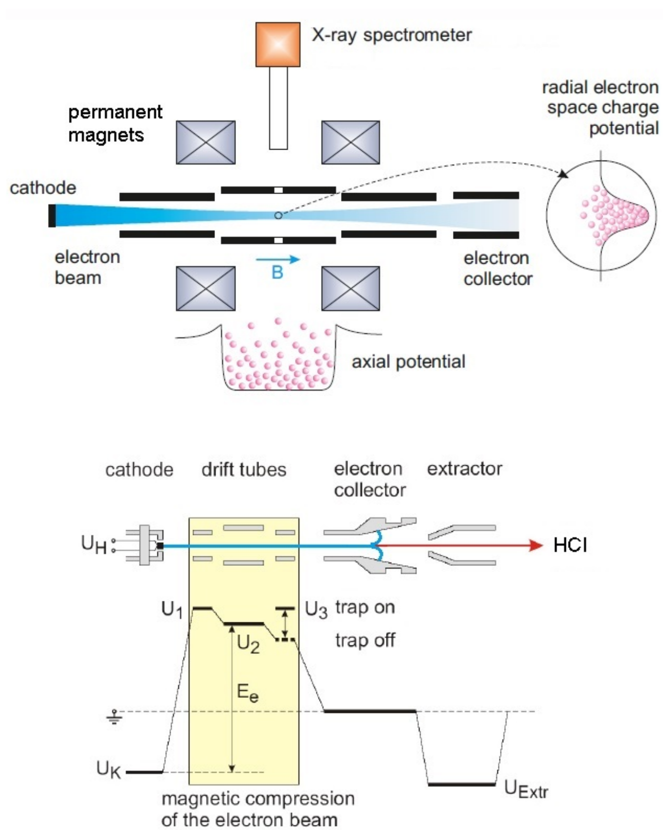

Fig. 2. Scheme of the Dresden EBIT (DREEBIT Co.) [2].

three drift tubes. These drift tubes are forming the electric field which traps ions. The electron beam ends in a water cooled collector. The electron beam is compressed by an axially symmetric magnetic field up to necessary electron density for production of highly charged ions. Magnetic field is created and formed by two toroidal permanent magnets. The electron beam is a heart of the apparatus: it works as ionization medium, electron source for atomic processes and, due to its negative space charge potential, as radial trapping potential for positively charged ions. Axial trapping is generated by the drift tubes. The extraction of ions is realized by a short-time lowering of the third drift tube voltage offset. Electron energy is determined by the accelerating potential between the cathode (electron source) and the electrode (anode) in the central part of the trap. Observation of the atomic processes, which take place in the trap, is based on the X-ray detection. The trap is equipped with an X-ray detector (XFlash 5030, Bruker Co.) with a resolution of about 130 eV (FWHM at 5.6 keV), placed perpendicular to the electron-beam axis at the distance of about 10 mm from the trap center (Fig. 2 (a)). Typical vacuum conditions in the trap are in the region of 10^{-10} mbar.

3. Argon charge-state evolution for different working parameters of the EBIT

As already mentioned, the distribution of the ion charge states plays a major role in order to explain the atomic processes in the EBIT. Different settings of the trap parameters determine the charge-state distribution of the ions in the trap. To some extent, it is possible to increase the concentration of the required highest ion charge states in order to enhance processes under consideration. One of the common procedures is called evaporative cooling [2, 4]. It is done by lowering of the trapping voltage and by using the appropriately low gas pressure. Low potential barrier is hardly seen by low charge-state ions, while highly charged ions are still trapped. Effects of the evaporative cooling for Ar can be observed with the Wien filter mounted just behind the trap working in the pulse mode (Fig. 3). This control method of the charge-state distribution requires relatively high-ion currents and determines the distribution just after the extraction from the trap. However, some experiments demand EBIT parameter settings which disfavor production of high-ion currents. Moreover, a detailed analysis of the processes under investigation may require a control of the charge-state distribution as a function of the ionization time, and the Wien filter method cannot be applied.

Therefore, we propose to control this charge-state distribution via analysis of the profile of the Ar K_α line. The goal is to use the Flexible Atomic Code calculations to reveal the charge-state evolution *in statu nascendi* in

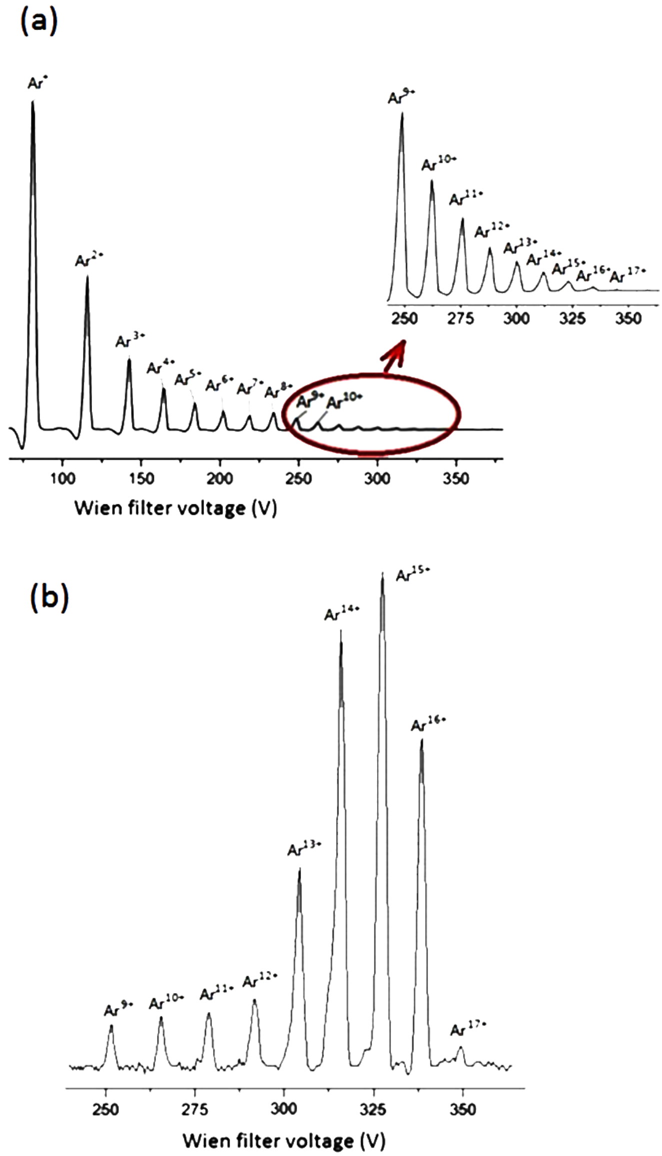

Fig. 3. An example of Ar charge-state distribution investigated with Wien filter in the pulse mode with 200 ms ionization time; (a) before and (b) after applying the evaporative cooling.

the trap. In Fig. 4 (a), as an example, results of the FAC calculations of the K_α-line position are shown for Ar^{12+} (C-like argon) where all the electronic configurations were taken into account. The K_α positions, shown in this figure, are weighted with the decay rates for each configuration. As demonstrated in Fig. 4 (a), this position variation, for a particular charge state, presents an asymmetric maximum-like behavior. These calculations were executed for ions Ar^{6+}–Ar^{16+}. Results of these calculations are collected in Fig. 4 (b). For all charge states, the average position value of all possible K_α transitions was estimated. The bars shown in Fig. 4 (b) are based on the analysis of the profile widths for each charge state. The same calculation procedure was performed for Ar^{17+}. For this particular ion, the K_α line has much higher energy (3320,6 eV) than for other charge states. This line demonstrates a transition of an electron from the L-shell to the K-shell when two vacancies in the K-shell are present (hypersatellite transition K^h_α).

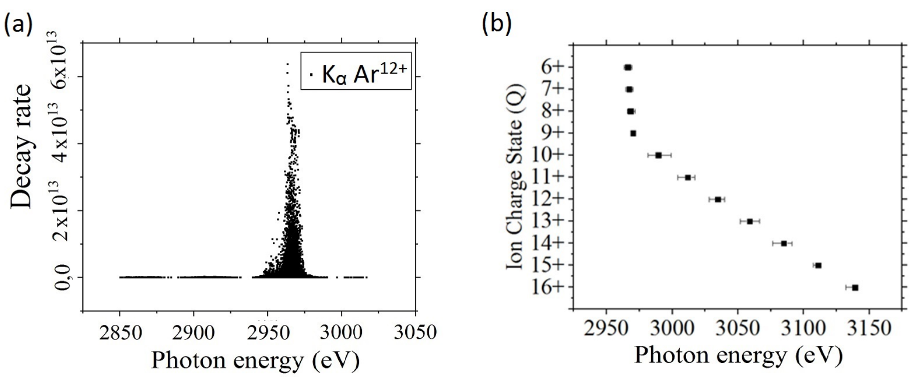

Fig. 4. (a) Variation of the K_α-line position weighted with the decay rates for all electronic configurations of Ar^{12+} (C-like) calculated with FAC; (b) Position of K_α line for different charge states ($^{6+}$–$^{16+}$) calculated as for $^{12+}$.

For data gathering, the TERX acquisition system [18] has been used. TERX allows us to collect time evolution of the X-ray data from the trap in 1 ms steps in a wide time range (till 10 s of ionization time). Figure 5 presents the idea of the charge-state distribution analysis as a function of the ionization time. Here, the K_α line data for a selected electron energy of 6440 eV are shown. The ionization time was changed in 1 ms steps from 25 ms to 1000 ms. Spectrum was cut into four intervals for different ionization times and integrated, as presented in Fig. 5. Then, based on the position of the K_α line for different charge states (Fig. 4 (b)) and the X-ray detector energy resolution, the distribution of charge states was fitted. For charge states lower than $Q = {}^{10+}$, position of the K_α line does not differ significantly (Fig. 4 (b)). Therefore, for these charge states, a single common line has been fitted. Figure 5 allows us to conclude that for long ionization times (longer than 250 ms) charge state of $Q = {}^{16+}$ is in favor. As expected, in the selected time window, the evaporative cooling is in action for the low potential well ($U_a - U_{b1} = 5$ V, Fig. 2) and low inlet gas pressure

(3.5×10^{-9} mbar). Here, the high charge states are strongly present, while the low charge states easily move from the trap. The low charge states are only present for low ionization times (below 250 ms).

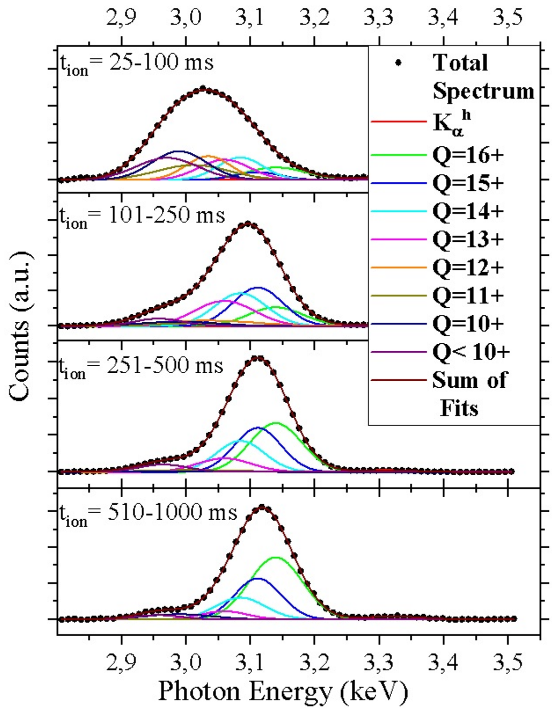

Fig. 5. Charge state distribution for four ionization time intervals (25–100 ms, 101–250 ms, 251–500 ms, 501–1000 ms), $E_e = 6440$ eV, gas pressure 3.5×10^{-9} mbar, trapping potential $U_a = 60$ V, $U_{b1} = 55$ V, $U_{b2} = 120$ V.

Action of the evaporative cooling helps to preliminary predict the shift of the dominant charge state in the EBIT plasma towards higher charge states. It was possible to demonstrate this effect by changing the running parameters of the trap. For data presented in Fig. 6, a deeper potential well ($U_a - U_{b1} = 95$ V) and a higher inlet gas pressure (6×10^{-9} mbar) was used in order to switch off the evaporative cooling. Here, the most populated charge state is shifted to $Q =^{14+}$ and the low charge states are strongly present regardless of the ionization time taken into consideration.

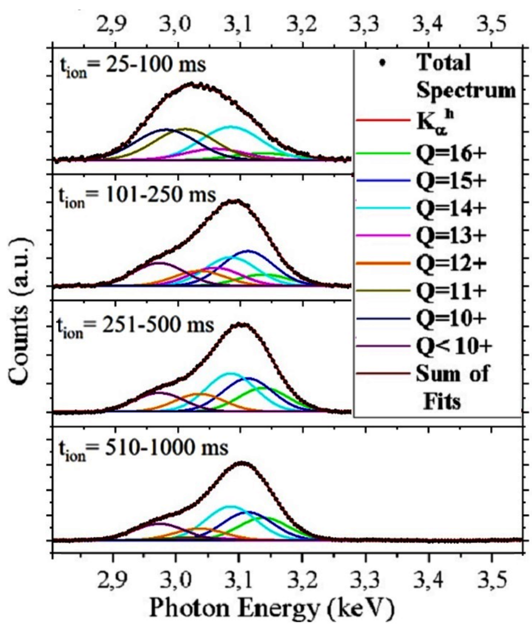

Fig. 6. Charge state distribution for four ionization time intervals (25–100 ms, 101–250 ms, 251–500 ms, 501–1000 ms), $E_e = 7000$ eV, gas pressure 6×10^{-9} mbar, trapping potential $U_a = 100$ V, $U_{b1} = 5$ V, $U_{b2} = 120$ V.

4. Conclusions

In this paper, an effective tool for the investigation of the time-dependent charge-state distribution of the Ar EBIT plasma has been proposed. The method is based on the analysis of the K_α-line profile. In particular, the line position plays here the most important role. The presented calculations were performed by using the Flexible Atomic Code. Results of this calculations were compared with experimental data. By means of this new diagnosis tool, the variation of the running EBIT parameters shows, successfully, the expected influence of the evaporative cooling. The proposed method is still to be completed with calculations which take into account the population probabilities of the electronic configurations generated by the electron–ion interaction. One has to remember that the observed K_α radiation is a fingerprint of the relaxation processes of the excited states formed via electron impact ionization and completed by rare multi-electron processes. A better understanding of the evolution, both of the ion charge-state distribution and of the electronic configuration, helps to plan a successful observation of rare atomic processes in the EBIT plasma.

REFERENCES

[1] G. Zschornack *et al.*, *Rev. Sci. Instrum.* **79**, 02A703 (2008).

[2] G. Zschornack, M. Schmidt, A. Thorn, CERN Yellow Report 007, 165–201, 2013.

[3] Y. Zou, J.R. Crespo Lopez-Urrutia, J. Ullrich, *Phys. Rev. A* **67**, 042703 (2003).

[4] C. Beilmann *et al.*, *Phys. Scr.* **T144**, 014014 (2011).

[5] C. Shah, P. Amaro, R. Steinruegge, *Phys. Rev. E* **93**, 061201 (2016).

[6] C. Shah *et al.*, *Phys. Rev. A* **92**, 042702 (2015).

[7] C. Shah *et al.*, *Astrophys. J. Suppl. Ser.* **234**, 27 (2018).

[8] W. Biela, A. Warczak, A. Mucha, A. Malarz, *X-Ray Spectrom.* **48**, 696 (2019).

[9] A. Burgess, *Astron. J.* **139**, 776 (1964).

[10] M. Bitter *et al.*, *Phys. Rev. Lett.* **71**, 1007 (1993).

[11] K. Widmann *et al.*, *Rev. Sci. Instrum.* **66**, 761 (1995).

[12] J.A. Tanis *et al.*, *Phys. Rev. Lett.* **53**, 2551 (1984).

[13] K.E. Zaharakis *et al.*, *Phys. Rev. A* **52**, 2910 (1995).

[14] C. Brandau *et al.*, *Phys. Rev. Lett.* **100**, 073201 (2008).

[15] V.A. Yerokhin, A.N. Artemyev, V.M. Shabaev, *Phys. Rev. A* **75**, 062501 (2007).

[16] I.I. Tupitsyn *et al.*, *Phys. Rev. Lett.* **117**, 253001 (2016).

[17] M.F. Gu, *Can. J. Phys.* **86**, 675 (2008).

[18] User Manual for EBIS S-Facility DREEBIT Co., 2012.